

OVERCOMING CHALLENGES IN LEVERAGING GANS FOR FEW-SHOT DATA AUGMENTATION

Christopher Beckham^{1,2,3}, Issam Laradji¹, Pau Rodriguez¹, David Vazquez¹, Derek Nowrouzezahrai^{2,4}, Christopher Pal^{1,2,3,†}

¹ServiceNow Research, ²Mila, ³Polytechnique Montreal, ⁴McGill University, [†]Canada CIFAR AI Chair

ABSTRACT

In this paper, we explore the use of GAN-based few-shot data augmentation as a method to improve few-shot classification performance. We perform an exploration into how a GAN can be fine-tuned for such a task (one of which is in a *class-incremental* manner), as well as a rigorous empirical investigation into how well these models can perform to improve few-shot classification. We identify issues related to the difficulty of training such generative models under a purely supervised regime with very few examples, as well as issues regarding the evaluation protocols of existing works. We also find that in this regime, classification accuracy is highly sensitive to how the classes of the dataset are randomly split. Therefore, we propose a semi-supervised fine-tuning approach as a more pragmatic way forward to address these problems.

1 INTRODUCTION

In the past decade, deep learning has demonstrated an immense level of success under many tasks and data modalities (Krizhevsky et al., 2012; LeCun et al., 2015; He et al., 2016). However, the issue of deep neural networks being highly data inefficient has been well established (Krizhevsky et al., 2012; Srivastava et al., 2014; Zhang & Yang, 2017; Tan et al., 2018), and this can be well accentuated by the fact that for some domains, obtaining a sufficient amount of labelled data can be laborious and expensive. Because this issue limits the real-world applicability of deep neural networks, an active area of research is in figuring out how to make these models transfer or learn better on underrepresented datasets. One of the very subfields that addresses this, few-shot learning, is centered around training models that are able to adapt to novel tasks which contain extremely few labelled examples.

Few-shot learning as a field is rather broad (Wang et al., 2020), and many techniques can be seen as incorporating prior knowledge into either the data, the model/architecture, or the algorithm in order to make the learning process more sample efficient. For example, this may be in the form of multitask learning (Caruana, 1997; Zhang & Yang, 2017) where the learning of a few-shot task can be augmented by learning other relevant tasks with more data, or in embedding learning (Bertinetto et al., 2016; Sung et al., 2018; Vinyals et al., 2016) where a low-dimensional metric space is learned to be able to easily facilitate comparisons between unseen classes. In terms of algorithmic few-shot learning, meta-learning (Finn et al., 2017; Ravi & Larochelle, 2016), i.e. *learning how to learn*, can be used to learn more sample efficient optimisers.

In this paper we specifically focus on the *data* aspect of few-shot learning, which at its core leverages some form of data augmentation to augment a small set of examples into a much larger set, one that is more amenable to the size of deep neural networks. In particular, we wish to explore this data augmentation in the form of generative models, where the goal is learning how to generate samples that are indistinguishable from ones from the few-shot task of interest. Specifically, in this paper we explore data augmentation-based few-shot learning with one of the more widely used generative models in the literature, the *generative adversarial network* (GAN) (Goodfellow et al., 2014), and detail our findings and challenges in using such a class of models. The very nature of these difficulties also means that many negative findings will be presented in this work. Concretely, our contributions are as follows:

- We explore the entire few-shot data augmentation pipeline, where the goal is to pre-train a GAN on some set of source classes, fine-tune it on very few examples of target classes, and have it be able to generate new images from those classes to maximise generalisation performance of a pre-trained classifier that is also fine-tuned to predict those target classes. Unlike previous works (Antoniou et al., 2017; Hong et al., 2020a;b), we specifically fine-tune our GAN on novel classes rather than try to generate from them in ‘zero shot’ fashion.
- We perform a rigorous empirical evaluation (over different randomised splits of the dataset, or *dataset seeds*) into how well few-shot data augmentation can perform. We highlight the difficulty of such a task, explain

limitations with the empirical evaluation of existing work, and propose a more pragmatic strategy involving semi-supervised GAN fine-tuning.

- As a side contribution, we propose a simple GAN fine-tuning strategy which allows it to learn new classes in a class-incremental manner, without catastrophic forgetting of old ones. This may be of interest to those working in the intersection of generative modelling and *generalised* few-shot learning.

1.1 FEW-SHOT DATA AUGMENTATION PIPELINE

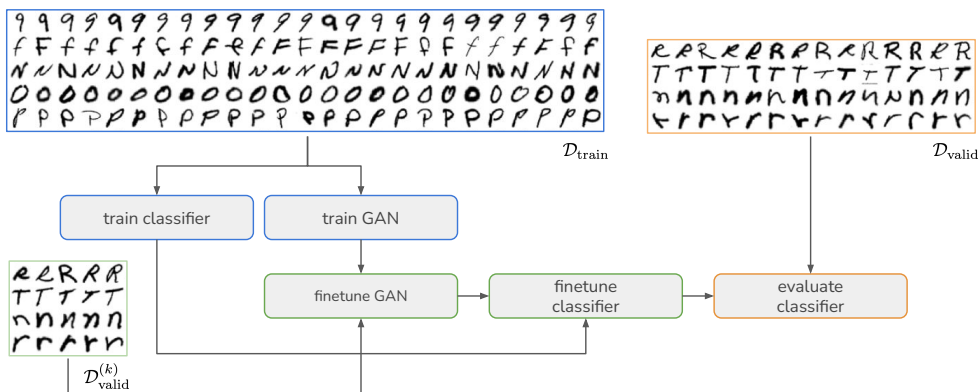


Figure 1: The few-shot data augmentation pipeline. Each block is described in Section 1.1.

Our few-shot data augmentation pipeline is illustrated in Figure 1. First, we divide our dataset into a training set $\mathcal{D}_{\text{train}}$, validation set $\mathcal{D}_{\text{valid}}$, and test set $\mathcal{D}_{\text{test}}$, where $\mathcal{Y}_{\text{train}} \cap \mathcal{Y}_{\text{valid}} = \emptyset$ and $\mathcal{Y}_{\text{valid}} = \mathcal{Y}_{\text{test}}$. Since the test set is simply just a held-out part of the validation set, we can think of the training and validation sets our *source* and *novel* (target) classes, respectively. The few-shot setting arises when, in addition to our large training set of source classes, we are given a very small subset of the novel classes in the validation set, which are called the ‘supports’ $\mathcal{D}_{\text{valid}}^{(k)}$. There are only k of these supports per class. Essentially, we would like to train a generative model on $\mathcal{D}_{\text{train}}$, fine-tune it on the very small set of examples defined in $\mathcal{D}_{\text{valid}}^{(k)}$, and have it be able to generate examples that are hopefully indistinguishable from those in the validation set $\mathcal{D}_{\text{valid}}$, which will be used to evaluate the quality of the generative model. Concretely, we would like to fine-tune a classifier – one that was originally trained on the source classes – to the novel classes, using the GAN to augment $\mathcal{D}_{\text{valid}}^{(k)}$ with more examples. Generalisation performance would then be evaluated on the validation set, and finally at the end on the test set. We precisely describe each stage as follows:

1. Section 2.1: pre-train a classifier on $\mathcal{D}_{\text{train}}$ which estimates $p(\mathbf{y} \in \mathcal{Y}_{\text{train}} | \mathbf{x})$. This classifier will eventually be fine-tuned to adapt to the new classes in $\mathcal{D}_{\text{valid}}$.
2. Sections 2.2 and 2.3: train a conditional GAN on $\mathcal{D}_{\text{train}}$, where we learn a conditional generative model $p_G(\mathbf{x} | \mathbf{y} \in \mathcal{Y}_{\text{train}})$. When this is completed, fine-tune it on the support set $\mathcal{D}_{\text{valid}}^{(k)}$, which will allow generation for the novel classes $p_G(\mathbf{x} | \mathbf{y} \in \mathcal{Y}_{\text{valid}})$.
3. Use the fine-tuned GAN to generate new examples for each class. These examples will be concatenated with the original support set $\mathcal{D}_{\text{valid}}^{(k)}$ to produce an ‘augmented’ set which we denote $\tilde{\mathcal{D}}_{\text{aug}}^{(k)}$.
4. Section 4: Lastly, take the pre-trained classifier, replace its output probability distribution to be over the novel classes $p(\mathbf{y} \in \mathcal{Y}_{\text{valid}} | \mathbf{x})$ and fine-tune it by using $\tilde{\mathcal{D}}_{\text{aug}}^{(k)}$ as the training set and perform model selection (hyperparameter tuning) on $\mathcal{D}_{\text{valid}}$. The best model is evaluated on $\mathcal{D}_{\text{test}}$, which is the unbiased measure of generalisation performance.

Because the few-shot setting requires us to adapt our models to novel classes with very small amounts of data, the evaluation can be highly sensitive to how the dataset is split. Furthermore, it may also be sensitive to what classes comprise source classes (those in the training set) and what classes comprise novel classes (those in the validation or test set). Because of this, almost all quantitative results in this paper are averages over many randomised splits of the dataset in order to produce reliable estimates of uncertainty. This is illustrated in Figure S13.

2 PROPOSED METHOD

The following subsections describe our method to address the steps described in Section 1.1.

2.1 CLASSIFIER PRE-TRAINING

Before we train our generative model, we need to train a classifier which can easily be adapted to any new classes we encounter. To do this, we first need to train it on a large dataset where there exists many examples per class, so that the features learned are robust and reliable. In our case, this is the training set $\mathcal{D}_{\text{train}}$.

The classifier we train is a ResNet-50 (He et al., 2016) initialised from scratch, trained with ADAM (Kingma & Ba, 2014) using learning rate 1×10^{-4} and moving average coefficients $\beta = (0.9, 0.999)$. The training set is split into a 95%-5% split, with the latter forming an internal validation set for early stopping. We train this classifier with a moderate amount of data augmentation, which can comprise randomly-resized crops anywhere between 70% to 100% of the original image size, and random rotations anywhere between -10 and 10 degrees. We simply train the classifier using the small internal validation set as an early stopping criteria.

2.2 GENERATIVE ADVERSARIAL NETWORKS

The generative adversarial network (Goodfellow et al., 2014) we use here is based on the projection discriminator proposed by Miyato & Koyama (2018), with a slight modification to make it more similar to the recently proposed StyleGAN class of models (Karras et al., 2018).¹ In StyleGAN, rather than the latent code being fed directly as input to the generator network, the input is instead a learnable constant tensor h_0 whose progressively growing representation is modulated by the latent code, via adaptive instance normalisation. This decision was made to more easily facilitate fine-tuning to new classes, since their layers comprise a relatively small number of learnable parameters. However, it has also been shown in Karras et al. (2018) that this particular architecture is superior to traditional architectures in terms of image quality and disentanglement.

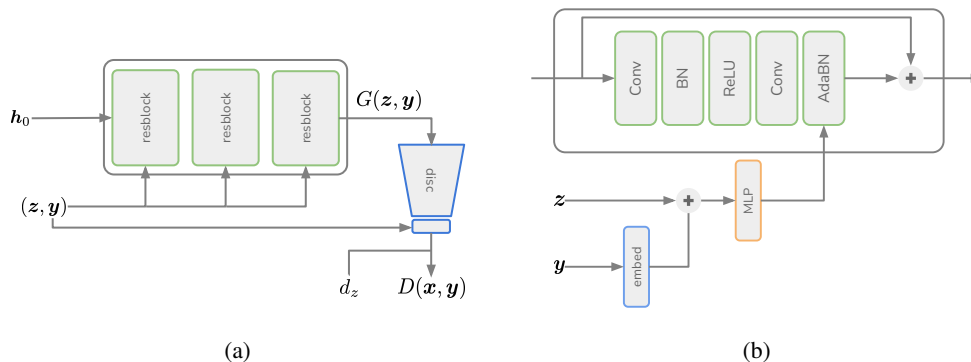


Figure 2: **Left:** overview of both the generator and discriminator. **Right:** The residual block used for the generator. The label y 's embedding is extracted and concatenated with the latent code to produce scale and shift coefficients for the second (last) batch normalisation layer. The addition symbol for the (z, y) part of the architecture indicates tensor concatenation.

We train a conditional GAN which comprises two networks: the generator $G(z, y)$ and discriminator $D(x, y)$, where $z \sim p(z)$ is the latent code (corresponding to image style) and y is the label (corresponding to image content, i.e. the digit). $p(z)$ here is simply an isotropic Gaussian. In terms of label conditioning, we utilise embedding layers that map indices from the label distribution $p(y)$ to codes which are concatenated with the latent codes z , which in turn are used to modulate residual blocks in the generator. This is illustrated in Figure 2. The objective function we use is the

¹The decision to build off of projection CGAN was simply due to time reasons. However, StyleGAN also has extra complexity due to a more sophisticated training algorithm (e.g. multi-resolution, mixing regularisation) and such complexity may not be necessary for a low-resolution toy dataset like EMNIST.

non-saturating logistic loss originally proposed in Goodfellow et al. (2014):

$$\min_D \mathcal{L}_D = -\mathbb{E}_{\mathbf{x}, \mathbf{y} \sim p(\mathbf{x}, \mathbf{y})} \log [D(\mathbf{x}, \mathbf{y})] - \mathbb{E}_{\mathbf{z} \sim p(\mathbf{z}), \mathbf{y} \sim p(\mathbf{y})} \log [1 - D(G(\mathbf{z}, \mathbf{y}), \mathbf{y})] \quad (1)$$

$$\min_G \mathcal{L}_G = -\mathbb{E}_{\mathbf{z} \sim p(\mathbf{z}), \mathbf{y} \sim p(\mathbf{y})} \log [D(G(\mathbf{z}, \mathbf{y}), \mathbf{y})], \quad (2)$$

where $D = \text{sigm}(d(\cdot))$. In practice, we experienced an issue where the GAN would exhibit serious mode dropping. This appears to be because of our use of a learnable constant as input to the network, though it is currently unclear what architectural choices in StyleGAN mitigate this. To fix this, we utilise the InfoGAN (Chen et al., 2016) loss where the discriminator has to also predict the latent code \mathbf{z} from the generated image $G(\mathbf{z}, \mathbf{y})$, which can be used to maximise mutual information between the generated image and \mathbf{z} . This extra loss is $\|d(G(\mathbf{z}, \mathbf{y}))_{\mathbf{z}} - \mathbf{z}\|^2$ and is minimised wrt both networks and is weighted by coefficient γ , where $d(\cdot)_{\mathbf{z}}$ is a \mathbf{z} prediction branch that stems off the main backbone of d . We suspect this loss may have a similar effect to the minibatch standard deviation layer in StyleGAN, which allows the discriminator to distinguish between real/fake based on minibatch statistics. We found that our InfoGAN loss does not have to be anywhere close to zero for it to have its intended effect of mitigating mode dropping. We train with ADAM (Kingma & Ba, 2014) parameters $\beta = (0.0, 0.9)$, $\text{lr} = 2 \times 10^{-4}$, InfoGAN coefficient $\gamma = 100$, with a G:D update ratio of 1:5.

For early stopping, we monitor the FID (Heusel et al., 2017) between our generated samples and training set. More specifically, we randomly sample $N = 5000$ examples from the training set to compute the statistics of the reference distribution, and also randomly sample $N = 5000$ labels to produce the same number of conditionally-generated samples.

2.3 FINE-TUNING

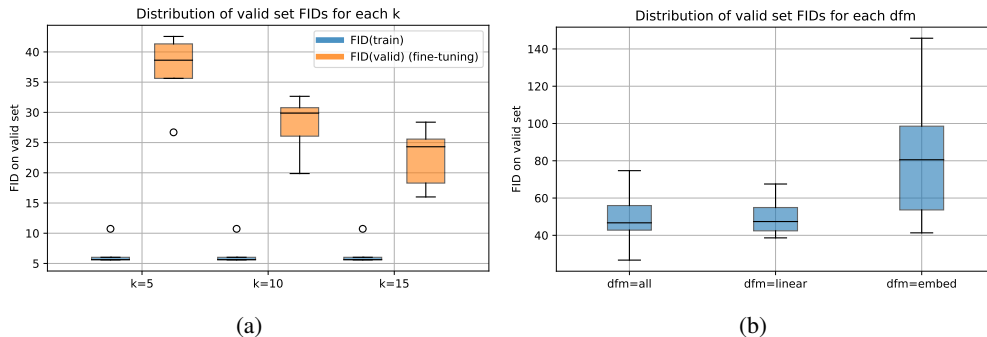


Figure 3: **Left:** For each k , we show the distribution of FID valid set scores (over dataset seeds) when the GAN is fine-tuned on the support set $\mathcal{D}_{\text{valid}}^{(k)}$. For each of these k , the training set FID is shown as blue as a reference. **Right:** the distribution of FID valid set scores (over dataset seeds and gfm modes) for different dfm modes.

When GAN training has completed, we need to figure out how to best fine-tune it on our support set, which contains very few examples (only k per class). Here, by ‘fine-tuning’, we mean optimising the same losses as we did earlier (i.e. playing the adversarial minimax game between G and D), as opposed to only fine-tuning the generator with non-adversarial losses (such as in Li et al. (2019)). This is a difficult task because we may risk overfitting if we try and optimise too many parameters in both the generator and discriminator. For our fine-tuning strategy, we found that the best strategy is to optimise *only the embedding layers* in G and, quite surprisingly, to optimise for *all* parameters in D , using the same adversarial losses and the same InfoGAN coefficient γ . In order to facilitate new classes, all that is required is for new indices (rows) to be added to each and every embedding layer’s matrix in both networks.² In Figure 3a we show the distribution of *validation set FIDs* (by generating samples on the *novel* classes) as a function of k . Perhaps not surprisingly, as k gets larger we are able to generate samples that progressively become more representative of those in the validation set. Here, we also show the FID on the training set (before fine-tuning) as a reference.

For the sake of comparison, we also measure performance when considering different ways in which D can also be finetuned, which we denote as dfm (‘D finetuning mode’). For a projection CGAN the discriminator logits can be

²Implementation-wise, this is not necessary as we simply assume that we know the total number of classes beforehand (train+valid+test) and initialise the embedding matrix to have precisely this many rows.

written as $d(\mathbf{x}, \mathbf{y}) = \mathbf{y}^T \mathbf{V} \cdot \phi(\mathbf{h}) + \psi(\phi(\mathbf{h}))$, where $\mathbf{h} = f_D(\mathbf{x})$ is the output of the discriminator’s backbone and \mathbf{V} is the embedding matrix that maps a (one-hot encoded) label to its embedding. From this equation, we can devise three ways in which D could be finetuned: $dfm=embed$ corresponds to only updating $\{\mathbf{V}, d(\cdot)_z\}$, $dfm=linear$ corresponds to updating $\{\mathbf{V}, \phi, \psi, d(\cdot)_z\}$, and $dfm=all$ corresponds to updating the backbone f_D as well. We can also define the ‘G finetuning mode’ (gfm) in a similar manner, with $gfm=embed$ denoting that we only update the embedding matrix per residual block, and $gfm=linear$ denoting both the embedding matrix and the MLP which produces adaptive instance norm parameters. Here though we omit $gfm=all$ as an option since we did not find it performed well. In Figure 3b we plot FID on the validation set for each of the three dfm modes, with the distribution of FIDs being computed over both dataset seeds and gfm . We can see that $dfm=embed$ performs the worst, and surprisingly, not much difference between $dfm=all$ and $dfm=linear$. We find this to be an interesting result given it is the opposite of ‘Freeze-D’ (Mot et al., 2020), whose work found the best results in fine-tuning *all* of G and just the later layers of D .

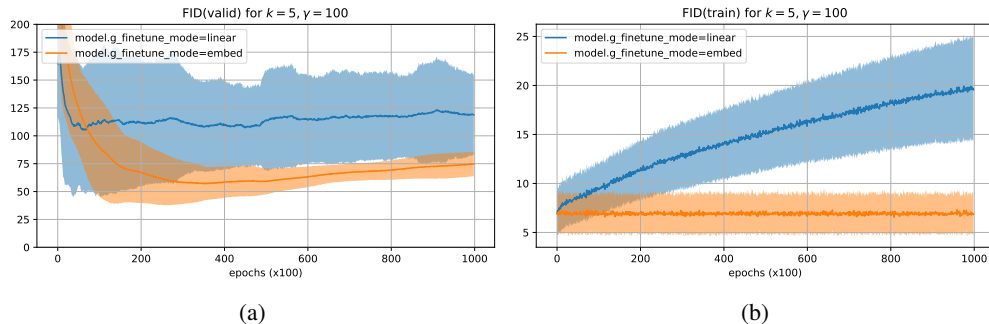


Figure 4: **Left:** FID between generated samples on the valid classes and the validation set, for GAN fine-tuning (Section 2.3) (lower FID is better). The orange curve corresponds to our proposed fine-tuning mode for G (embedding layers only, i.e. $gfm=embed$) versus also fine-tuning the MLPs which produce adaptive batch norm coefficients (i.e. $gfm=linear$, see Figure 2b). Shaded regions (variance) is over all possible dfm ’s (*all*, *linear*, or *embed*). **Right:** same as left but FID is computed between samples on the training classes and the training set. Here, we can see that fine-tuning only the embedding layers in G does not result in catastrophic forgetting in how to generate samples for training classes.

In Figure 4 we present some additional results comparing the fine-tuning mode of G , which we denote as gfm . We compare fine-tuning just the embeddings in G ($gfm=embed$) versus also fine-tuning the MLPs that take part in adaptive batch normalisation ($gfm=linear$, see Figure 2b). It can be seen that with $gfm=embed$, validation set FIDs are superior on average and that the training set FID does not degenerate over time (Figure 4b).

One may wonder in what situations does it simply suffice to only finetune the embedding layers in G and have it perform well for generation. We recognise that this is highly dependent on both the architecture and datasets used. Unlike the more ambitious task of domain transfer, here our source and target classes can be seen as coming from the same overall distribution $p(\mathbf{x})$, but with different sets of conditioning labels $\mathbf{y} \in \mathcal{Y}_{train}$ or $\mathbf{y} \in \mathcal{Y}_{valid}$ for the conditional distribution $p(\mathbf{x}|\mathbf{y})$. If source classes in the training set share very similar factors of variation to target classes in the validation or test set, then we would expect the network to generalise to those new classes with minimal modification to the original weights of the network. A real world example of this would be finetuning from the source classes {cat, dog} to {tiger, fox}, with many common factors of variation shared between the two (four legs, fur, tails, and so forth).

3 RELATED WORK

A very closely related work is DAGAN (Antoniou et al., 2017). The authors proposed training a GAN where the discriminator is trained to distinguish pairs of images, rather than images conditioned on labels. This means that D is trained to distinguish between a same-class tuples from the real distribution $(\mathbf{x}_1, \mathbf{x}_2)$ and a pair from the fake distribution, where one of the elements is generated $(\mathbf{x}, \tilde{\mathbf{x}})$, where $\tilde{\mathbf{x}} = G(r(\mathbf{x}), \mathbf{z})$. In this case, $r(\mathbf{x})$ is an encoder network and G is the corresponding decoder. The authors motivate this by wanting a discriminator that can naturally generalise to new classes, since it is not explicitly conditioned on a label. For their generator network, $r(\mathbf{x})$ is meant to infer (without any explicit label supervision) the ‘content’ of the image, while \mathbf{z} serves as the ‘style’ which is simply noise injected from a prior. However, upon attempting to reproduce this model we found a major deficiency, in that the trained decoder G ignores $r(\mathbf{x})$ completely, i.e. $G(r, \mathbf{z}) \approx G(\mathbf{0}, \mathbf{z})$. This seems most likely attributable to the fact there is no supervision at all for $r(\mathbf{x})$, i.e. a reconstruction error or InfoGAN-style losses to ensure that both \mathbf{z} and $r(\mathbf{x})$ are used by the network. Such losses do not appear to be present in the paper. Furthermore, from the results it is

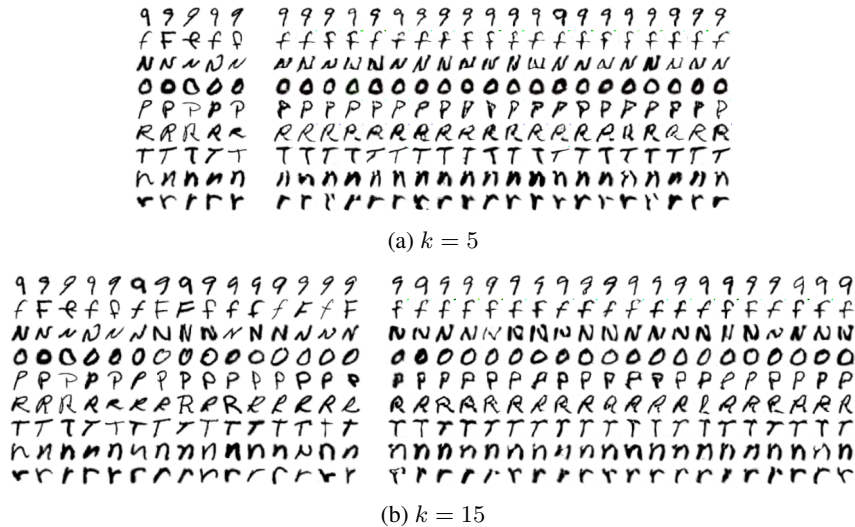


Figure 5: Generated examples from the fine-tuned GAN for $k = 5$ (5a) and $k = 15$ (5b). In each subfigure, the left panel shows the supports $D_{\text{valid}}^{(k)}$ and the right panel shows the generated images (20 examples per class). For additional examples, see Figure S11.

unclear if the method would outperform a discriminator that conditions on the class label for the training set. Despite this, a big difference between their works and ours is that they try to perform zero-shot generation with respect to the *generative model*, since it itself is not fine-tuned on the novel classes. In our own preliminary experiments however a model we trained similar to DAGAN, we found that when we tried to generate images from novel classes with $r(\mathbf{x})$, there was a strong bias towards it generating images that looked like classes from the training set.

F2GAN (Hong et al., 2020b) proposes an adversarially-augmented autoencoder where k -way mixup (Zhang et al., 2017; Verma et al., 2019a) is performed between the latent features of k images, coupled with an attention module to patch up discrepancies in the image (hence ‘fusing and filling’). Unlike DAGAN, a conditional discriminator is used which conditions on labels. In this work, a ‘mode seeking’ loss is proposed to ensure that, for the same pairs of images, different mixing coefficients correspond to sufficiently diverse images. While an ablation study was performed to justify each component/loss that was added, this was not done for any of the datasets for which few-shot classification was performed and therefore it is unclear which components of the model are most influential. Like DAGAN, there is no finetuning on the support set of novel classes, and the model is expected to perform zero-shot generation.

One crucial difference between what we propose and both of these works is that ours requires the generative model to be fine-tuned on novel classes. Wertheimer et al. (2020) argue that generative models such as GANs and VAEs have extreme difficulty generalising to novel classes in a ‘zero-shot’ manner (i.e. without fine-tuning) due to the fact that the training of either models enforces that all plausible regions in the space of the prior distribution decode into plausible samples from the training distribution. They argue that unlike their probabilistic variants, *deterministic* autoencoders are fit for few-shot generalisation because of this lack of rigidity, and propose a novel mixup scheme to ensure interpolations between images in novel classes do not produce images biased towards the training set. We argue that in the case of VAEs however, it depends on the trade-off between the two competing losses that comprise the evidence lower bound (ELBO), which is the likelihood + KL (between posterior and prior). The likelihood (reconstruction error) encourages a bijective mapping between \mathcal{X} and \mathcal{Z} , which allows it to generalise to novel inputs. The KL loss acts as a regularisation to make the posterior $q(\mathbf{z}|\mathbf{x})$ indistinguishable from the prior $p(\mathbf{z})$, and in the extreme case would bottleneck the capacity of the network and map many distinguishable inputs to the same mode, which is the opposite to the intended goal of the likelihood term (Esmaeili et al., 2019). An extensive literature surrounds the trade-off between these two terms (Burgess et al., 2018; Esmaeili et al., 2019; Mathieu et al., 2019). A similar analogy could be made for autoencoders with adversarial losses such as F2GAN, where we can imagine the KL loss being replaced with an ‘adversarial’ divergence between images created by the decoder and images from the training distribution (Berthelot et al., 2018; Sainburg et al., 2018; Beckham et al., 2019). Too much weighting on this term would produce a strong bias in the decoder to ensure *all* images are indistinguishable from those from the training distribution, potentially to the detriment of it being able to generate new samples from inputs coming from unseen classes. This seems to explain why F2GAN contains a multitude of losses to try and encourage sample diversity, though as we have stated, in our work we would prefer to simply fine-tune a GAN to novel classes directly.

One major issue in comparing these papers’ results is that there has not been a standardised way in which the data is split for training and evaluation. DAGAN is the most rigorous in its evaluation, utilising a ‘source’ domain (training set), a ‘validation’ domain (validation set), and a ‘target’ domain (test set). For the validation and testing sets, k examples per class are held out in each, which can be thought of as the support sets for both the validation and testing sets, respectively. These support sets are leveraged by the generative model to create more examples for their respective classes. In DAGAN, the validation set is used to tune the number of synthetic examples that should be generated per class. Conversely, in F2GAN there appears to be no mention of a validation set, and the data is simply split between a training domain and a testing domain. Because of hyperparameter tuning, it is likely performance estimates are biased, and this will be discussed in further detail in Section 4.

There are many works which involve the fine-tuning of GANs. Robb et al. (2020) proposes a new method to finetune a pre-trained StyleGAN (Karras et al., 2018) in the few-shot regime by tuning only the singular values of both networks. Karras et al. (2020) propose a trick to mitigate discriminator overfitting to improve StyleGAN2 training, and present transfer learning results in the context of domain adaptation. Such tricks could be leveraged to potentially improve our results in Section 2.3. The aforementioned work of Wertheimer et al. (2020) also performs few-shot data augmentation but in the context of domain adaptation, where one is interested in mapping between datasets. Casanova et al. (2021) propose ‘instance conditioned’ GANs that condition on pre-trained self-supervised embeddings rather than class labels, and demonstrate impressive zero-shot transfer to other datasets, simply by computing embeddings over these other datasets. While these works undoubtedly present impressive results on larger and more ambitious datasets, none of them have examined a few-shot pipeline where the goal is to generate images to improve a downstream task directly, such as classification performance. These works instead primarily report image similarity metrics computed on their generated images.

A closely related subfield is that of few-shot hallucination (Hariharan & Girshick, 2017), which may also involve using generative models (Li et al., 2020) to ‘hallucinate’ (generate) additional examples for novel classes, but in latent space instead of input space. Similar to our procedure, these hallucinated latent samples are combined with real latent samples to make one larger dataset. In principle, our method could be adapted to generate latent codes (with respect to a latent distribution), but this is left to future work. Lastly, while we do not consider meta-learning here, our few-shot pipeline could be framed as an end-to-end approach under that paradigm. There are numerous works combining generation with few-shot classification (Zhang et al., 2018; Wang et al., 2018; Chen et al., 2019; Verma et al., 2019b).

4 EXPERIMENTS AND RESULTS

Here, we present the results of our classifier fine-tuning experiments on both the validation and test sets, over five randomised dataset seeds (splits) on the balanced version of the EMNIST dataset (Cohen et al., 2017). For each dataset seed, the training set and validation sets comprise of 38 and 9 randomly sampled classes (without replacement), respectively. Each class comprises 2800 examples, with 80% being allocated for validation and 20% for testing. The support set is a subset of the validation set, with only k examples per class. The test set shares the same classes as the validation set but is held out and is only used for unbiased evaluation after model selection has been performed over the validation set.

While we already have a fine-tuned GAN which can generate images from the novel classes, we also need to fine-tune the classifier which was originally trained on the source classes (Section 2.1). To do this, we simply freeze all of its parameters and replacing its output (logits) layer with a new layer which defines a probability distribution over either the validation classes $\mathcal{Y}_{\text{valid}}$ or the test classes $\mathcal{Y}_{\text{test}}$. Note that unlike with generalised few-shot learning, here we are not interested in maximising performance over both the old and new classes – we simply wish to maximise performance over the latter. Here, we use the same parameters for ADAM as described in Section 2.1 but lower the learning rate to 2×10^{-5} , and train for 30k epochs. We describe our experiments and their corresponding hyperparameters as follows:

- **Baseline:** we fine-tune the pre-trained classifier on $\mathcal{D}_{\text{valid}}^{(k)}$. We run two experiments for this, one with and without traditional data augmentation applied. For the data augmentation experiment, we tune over the minimum random resized crop size $\text{minScale} \in \{0.2, 0.4, 0.6, 0.8\}$.
- **Mixup:** use mixup in input space (Zhang et al., 2017), where the mixing distribution $\text{Beta}(\lambda, \lambda)$ is a hyperparameter, and $\lambda \in \{0.1, 0.2, 0.5, 1.0\}$. This is done ‘on the fly’: for each minibatch seen during fine-tuning, input mixup is applied to both the images and their labels. minScale is fixed to 0.8 here.
- **Fine-tuned GAN:** Using the fine-tuned GAN, we pre-generate n_s new samples per class and combine these with the original supports $\mathcal{D}_{\text{valid}}^{(k)}$ to create $\tilde{\mathcal{D}}_{\text{aug}}^{(k)}$. Here, $n_s \in \{2, 5, 10, 20\}$ is a hyperparameter that we explore. minScale is also fixed to 0.8 here.

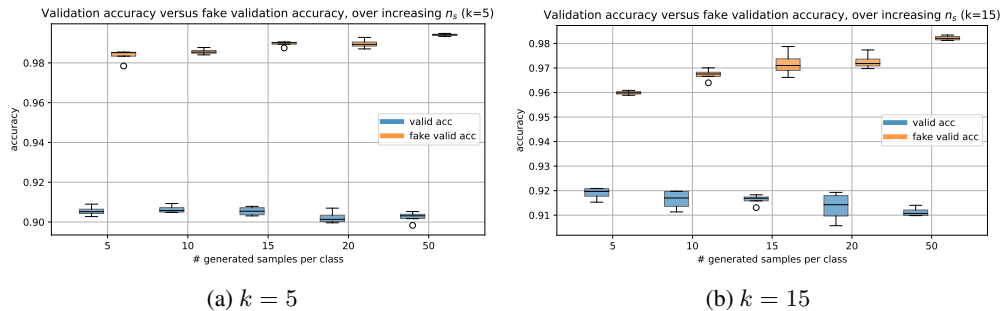


Figure 6: Boxplot showing validation accuracy (blue) and fake validation accuracy (orange) for different numbers of generated samples per class n_s . Fake validation accuracy is a held-out validation set generated by the GAN. It can be seen that as n_s increases, the actual validation accuracy decreases and fake validation accuracy increases. Results are shown over one dataset seed, with each boxplot being a distribution over the different sampling runs.

Table 1: Accuracy (%) of different methods on EMNIST on $\mathcal{D}_{\text{valid}}$. The separating bar distinguishes between results we have lifted from the F2GAN (Hong et al., 2020b) paper and our own results. These two groups of results are not directly comparable due to a variety of confounding factors in the experimental setup. In our results, uncertainty estimates are computed over five different randomised dataset splits (seeds) on the validation set. For each of these seeds, hyperparameter tuning was used to obtain the best result. The best hyperparameters can be found in Section S7.4.

Method	EMNIST		
	$k = 5$	$k = 10$	$k = 15$
F2GAN			
Baseline	83.64	88.64	91.14
w/ data aug.	84.62	89.63	92.07
FIGR (Clouâtre & Demers, 2019)	85.91	90.08	92.18
GMN (Bartunov & Vetrov, 2018)	84.12	91.21	92.09
DAWSON (Liang et al., 2020)	83.63	90.72	91.83
DAGAN (Antoniou et al., 2017)	87.45	94.18	95.58
MatchingGAN (Hong et al., 2020a)	91.75	95.91	96.29
F2GAN (Hong et al., 2020b)	93.18	97.01	97.82
ours			
Baseline	90.97 ± 4.62	92.68 ± 4.01	93.45 ± 3.69
w/ data aug.	91.27 ± 4.72	92.77 ± 4.06	93.47 ± 3.80
Input mixup (Zhang et al., 2017)	91.00 ± 4.39	92.68 ± 3.99	93.32 ± 3.68
Fine-tuned GAN	91.11 ± 4.62	92.85 ± 4.02	93.35 ± 3.79
+ semi-supervised (Sec. 5)	92.12 ± 4.34	93.27 ± 4.00	93.79 ± 3.72

We present our results in in Table 1. We can see that all results are characterised by non-negligible variances, especially when k is small. This can be problematic because it can diminish the statistical significance of any claims in performance gains. If we just consider the mean accuracy however, the data augmentation baseline performs best for $k = 5$ and $k = 15$ and our method performs best for $k = 10$. We found that validation accuracy is highly dependent on the number of generated samples per class n_s , and often times accuracy degrades when it is too high. We conjecture that this is because there is a fundamental mismatch between the distribution of GAN-generated images and those from the validation set (whose accuracy we wish to maximise), and this is leading to overfitting on the former. To validate this, we generate a held-out validation set from the same GAN that we generated the images from, which we call our ‘fake’ validation set. We can see in Figure 6 that as n_s increases, so does accuracy on our fake validation set, and this is negatively correlated with accuracy on the actual validation set. This clearly indicates we are indeed overfitting to the distribution induced by our GAN.

The results reported by F2GAN (Hong et al., 2020b) in the upper panel of Table 1 are indeed notable compared to ours for $k = 10$ and $k = 15$, but unfortunately their description of how the dataset was split is unclear and there are concerns with how principled this evaluation is. In their work, they describe EMNIST as comprising of 47 classes but with 28 being selected as training classes and 10 as testing, leaving 9 classes unaccounted for. In their preceding work MatchingGAN (Hong et al., 2020a), the dataset is split into 28-10-10 (i.e. train-valid-test) for a total of 48 classes, with 10 classes being used as a validation set for GAN training. The test set (10 classes) is used for classifier evaluation, with a small support set of k examples per class used by the GAN to generate additional examples. However, excessive

tuning of hyperparameters of the GAN (that is, the hyperparameters that directly control generation, e.g. the generation seed or number of generated samples per class n_s) and hyperparameters of the classifier can lead to biased estimates of performance on the test set, which is why we have also presented results on our test set in Table 2. In this table, we find that for all values of k , the data augmentation baseline performs the best in terms of mean accuracy, though like we have mentioned earlier, these results have relatively inflated variances which diminish their significance.

Another confounder is that MatchingGAN report artificially reducing the size of all classes in EMNIST to be 100 examples per class to mimic DAGAN’s setup, but it is not clear whether F2GAN has also done this. For reference, the only two splits of EMNIST with 47 classes are ByMerge and Balanced, with Balanced containing 2,800 examples per class and ByMerge containing anywhere between 2,961-44,704 examples per class, so this is an enormous reduction in dataset size. Such a reduction would be detrimental to both classifier pre-training and GAN training. While DAGAN’s evaluation protocol differs slightly to our work and the other works, they report 76% test set accuracy on EMNIST with $k = 15$ with this artificial reduction in examples per class. Lastly, for both MatchingGAN and F2GAN, the number of samples generated per class with the GAN was set to $n_s = 512$, which is extraordinarily large, considering that we obtain worse results on our validation set with anything more than $n_s = 5$, on average. Our results appears to corroborate that of DAGAN, whose authors report only tuning $n_s \in \{1, \dots, 10\}$. Because there are many subtle differences in the empirical evaluation between our work and the aforementioned ones, we simply defer the reader to Figures S13, S14, S15 for more information rather than enumerate all of these here.

Table 2: Results of selected experiments on the held-out test set $\mathcal{D}_{\text{test}}$. For each experiment and its dataset seed, the hyperparameters used for the test set evaluation correspond to the optimal hyperparameters found for the same corresponding experiment / seed on the validation set (e.g. # of epochs, α for input mixup, n_s for GAN).

Method		EMNIST		
		$k = 5$	$k = 10$	$k = 15$
ours	Baseline w/ data aug	90.65 \pm 4.52	92.22 \pm 4.19	93.02 \pm 3.94
	Input mixup (Zhang et al., 2017)	90.69 \pm 4.34	92.27 \pm 4.05	93.04 \pm 3.65
	Fine-tuned GAN	90.81 \pm 4.53	92.50 \pm 4.11	92.90 \pm 4.03
	+ semi-supervised (Sec. 5)	91.64 \pm 4.35	92.95 \pm 4.14	93.42 \pm 3.84

5 FURTHER DISCUSSION

One major limitation of using conditional GANs for data augmentation is that there is no way to leverage unlabelled data, which tends to be more abundant than labelled data. Another issue with our setup is that downstream performance is likely to only give practical gains for a very specific range of values for k . For example, when k is too small, there is a strong incentive for one to leverage GAN-based data augmentation since there are very few examples per class, but as we have demonstrated, fine-tuning a GAN is difficult precisely because of how few examples there are. Conversely, as k becomes larger, even if we could finetune a better GAN we would also expect there to be diminishing returns when it comes to improving classification performance over the baseline, since there are an abundant number of labelled examples per class. Therefore, having the ability to leverage unlabelled data seems like a more pragmatic endeavour since we could still experiment with small k but likely do a much better job at fine-tuning a better quality generative model over the new classes. Fortunately, it turns out that one can take the projection discriminator equation of Miyato & Koyama (2018) that we use and easily turn it into a semi-supervised variant. Recall from Section 2.3 that the output of the discriminator can be written as follows:

$$d(\mathbf{x}, \mathbf{y}) = \mathbf{y}^T \mathbf{V} \cdot \phi(\mathbf{h}) + \psi(\phi(\mathbf{h})), \quad (3)$$

with $\mathbf{h} = f_D(\mathbf{x})$, where f_D is the backbone of D , and $D = \text{sigm}(d(\cdot))$. From Miyato & Koyama (2018), this equation is the result of modelling the likelihood ratio of both the data and generative distributions:

$$f(\mathbf{x}, \mathbf{y}) = \log \frac{q(\mathbf{x}, \mathbf{y})}{p(\mathbf{x}, \mathbf{y})} = \log \frac{q(\mathbf{y}|\mathbf{x})q(\mathbf{x})}{p(\mathbf{y}|\mathbf{x})p(\mathbf{x})} = \log \frac{q(\mathbf{y}|\mathbf{x})}{p(\mathbf{y}|\mathbf{x})} + \log \frac{q(\mathbf{x})}{p(\mathbf{x})}, \quad (4)$$

where the last two terms here are modelled with their respective terms in Equation 3. From this, one can easily see that $d(\mathbf{x}) = \psi(\phi(\mathbf{h}))$ and that this is modelling the log ratio $q(\mathbf{x})/p(\mathbf{x})$, which is not a function of the label. From this, we can write the semi-supervised equations as:

$$\min_D \mathcal{L}_D = \mathcal{L}_D^{(\text{sup})} - \alpha \left[\mathbb{E}_{\mathbf{x} \sim p_u(\mathbf{x})} \log [D(\mathbf{x})] - \mathbb{E}_{\mathbf{z} \sim p(\mathbf{z}), \mathbf{y} \sim p(\mathbf{y})} \log [1 - D(G(\mathbf{z}, \mathbf{y}))] \right] \quad (5)$$

$$\min_G \mathcal{L}_G = \mathcal{L}_G^{(\text{sup})} - \alpha \left[\mathbb{E}_{\mathbf{z} \sim p(\mathbf{z}), \mathbf{y} \sim p(\mathbf{y})} \log [D(G(\mathbf{z}, \mathbf{y}))] \right], \quad (6)$$

where $\mathcal{L}_D^{(\text{sup})}$ and $\mathcal{L}_G^{(\text{sup})}$ are their respective terms in Equation 1, p_u denotes some unlabelled distribution (i.e. the validation set but with the labels ignored), and α controls the strength of the unsupervised part of the objective. Note that here the generator is not modified to perform unconditional generation – it simply has to fool both the conditional branch $d(\mathbf{x}, \mathbf{y})$ and unconditional branch $d(\mathbf{x})$. α should be carefully tuned here, as if it is too large then the generator may fail to generate class-consistent samples. We are not aware of any work which adapts the projection discriminator in this way, though Sricharan et al. (2017) proposed a semi-supervised CGAN variant which is conceptually similar to Equation 3. To train with this objective, we can simply consider fine-tuning using the entire validation set $\mathcal{D}_{\text{valid}}$ (without labels) for the unsupervised terms in Equation 5, in addition to the labelled support set $\mathcal{D}_{\text{valid}}^{(k)}$ for the supervised terms. In Figure 7 we show the distribution of FID scores obtained when we employ our semi-supervised variant, and also when we are able to tune α . We can see that the latter provides a very significant improvement in FID scores, and this improvement in sample quality is also reflected in Table 1, which achieves the best mean performance across the board.

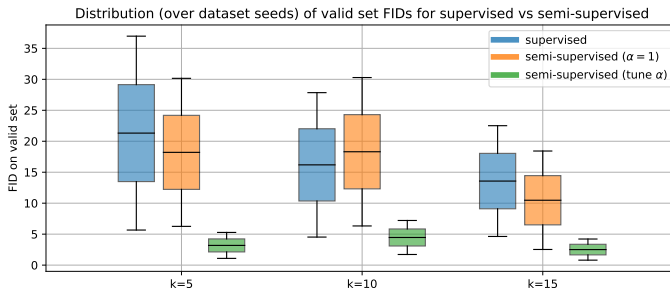


Figure 7: Comparison of FID scores on $\mathcal{D}_{\text{valid}}$ between supervised (Equation 1) and semi-supervised variant (Equation 5). ‘Tune α ’ refers to also tuning the α coefficient.

In general, we consider generative modelling in the few-shot regime to be a difficult task. All generative models present a trade-off (Xiao et al., 2021) between three criteria: sample quality, fast sampling, and mode coverage/diversity, with GANs tending to be problematic in the latter. Variational autoencoders (VAEs) on the other hand suffer from reduced sample quality but at the benefit of mode coverage. Score-based (Song et al., 2020) and denoising diffusion probabilistic models (DDPMs) (Sohl-Dickstein et al., 2015; Ho et al., 2020) appear to perform well in terms of both mode coverage and sample quality, and may be a more appealing alternative since its main bottleneck – sample generation – is only of concern if one wants to be able to generate samples in real-time, which is not a concern for us here. Of course, there is still the issue of training or fine-tuning a generative model on limited amounts of labelled data, but we believe a reasonable approach for the time being is through a semi-supervised approach, since unlabelled data is usually abundant.

Lastly, one potential issue we make note of is the discrepancy between using FID as an early stopping metric, which is not the same as the true metric we wish to optimise (classifier accuracy). This was done purely for pragmatic reasons, and our analysis could at least be made more meaningful by decomposing evaluation of our generated samples into precision and recall (Kynkäänniemi et al., 2019) (sample quality and mode coverage, respectively).

6 CONCLUSION

In this paper, we explored the use of generative adversarial networks to perform few-shot data augmentation in order to improve classification performance on EMNIST. While we qualitatively demonstrated the ability to finetune a GAN to generate examples from novel classes in the few-shot regime, it is difficult to leverage a large number of generated examples from the GAN to fine-tune a classifier because it can easily overfit to those examples. Such a phenomena is due to the fact that there is an inherent mismatch between the actual vs generative distribution of examples conditioned on those novel classes, and this effect is further exacerbated by how few examples are used. Furthermore, we found that classification performance is highly dependent on how classes are partitioned and this can induce significant variance, which is something not accounted for or presented in previous works. In order to mitigate this, we proposed a more pragmatic training setup that allows for unlabelled examples to be used for GAN fine-tuning (i.e. *semi-supervised fine-tuning*) and demonstrated gains in mean validation and test accuracy, as well as FID. Future work should entail validating this approach on natural image datasets, as well as considering more recent approaches in generative modelling.

REFERENCES

- Antreas Antoniou, Amos Storkey, and Harrison Edwards. Data augmentation generative adversarial networks. *arXiv preprint arXiv:1711.04340*, 2017.
- Sergey Bartunov and Dmitry Vetrov. Few-shot generative modelling with generative matching networks. In *International Conference on Artificial Intelligence and Statistics*, pp. 670–678. PMLR, 2018.
- Christopher Beckham, Sina Honari, Vikas Verma, Alex M Lamb, Farnoosh Ghadiri, R Devon Hjelm, Yoshua Bengio, and Chris Pal. On adversarial mixup resynthesis. *Advances in Neural Information Processing Systems*, 32:4346–4357, 2019.
- David Berthelot, Colin Raffel, Aurko Roy, and Ian Goodfellow. Understanding and improving interpolation in autoencoders via an adversarial regularizer. *arXiv preprint arXiv:1807.07543*, 2018.
- Luca Bertinetto, João F Henriques, Jack Valmadre, Philip Torr, and Andrea Vedaldi. Learning feed-forward one-shot learners. In *Advances in neural information processing systems*, pp. 523–531, 2016.
- Christopher P Burgess, Irina Higgins, Arka Pal, Loic Matthey, Nick Watters, Guillaume Desjardins, and Alexander Lerchner. Understanding disentangling in β -vae. *arXiv preprint arXiv:1804.03599*, 2018.
- Rich Caruana. Multitask learning. *Machine learning*, 28(1):41–75, 1997.
- Arantxa Casanova, Marlène Careil, Jakob Verbeek, Michal Drozdal, and Adriana Romero Soriano. Instance-conditioned gan. *Advances in Neural Information Processing Systems*, 34, 2021.
- Xi Chen, Yan Duan, Rein Houthoofd, John Schulman, Ilya Sutskever, and Pieter Abbeel. Infogan: Interpretable representation learning by information maximizing generative adversarial nets. *arXiv preprint arXiv:1606.03657*, 2016.
- Zitian Chen, Yanwei Fu, Yu-Xiong Wang, Lin Ma, Wei Liu, and Martial Hebert. Image deformation meta-networks for one-shot learning. In *Proceedings of the IEEE/CVF Conference on Computer Vision and Pattern Recognition*, pp. 8680–8689, 2019.
- Louis Clouâtre and Marc Demers. Figr: Few-shot image generation with reptile. *arXiv preprint arXiv:1901.02199*, 2019.
- Gregory Cohen, Saeed Afshar, Jonathan Tapson, and Andre Van Schaik. Emnist: Extending mnist to handwritten letters. In *2017 International Joint Conference on Neural Networks (IJCNN)*, pp. 2921–2926. IEEE, 2017.
- Babak Esmaeili, Hao Wu, Sarthak Jain, Alican Bozkurt, Narayanaswamy Siddharth, Brooks Paige, Dana H Brooks, Jennifer Dy, and Jan-Willem Meent. Structured disentangled representations. In *The 22nd International Conference on Artificial Intelligence and Statistics*, pp. 2525–2534. PMLR, 2019.
- Chelsea Finn, Pieter Abbeel, and Sergey Levine. Model-agnostic meta-learning for fast adaptation of deep networks. In *International Conference on Machine Learning*, pp. 1126–1135. PMLR, 2017.
- Ian J Goodfellow, Jean Pouget-Abadie, Mehdi Mirza, Bing Xu, David Warde-Farley, Sherjil Ozair, Aaron Courville, and Yoshua Bengio. Generative adversarial networks. *arXiv preprint arXiv:1406.2661*, 2014.
- Bharath Hariharan and Ross Girshick. Low-shot visual recognition by shrinking and hallucinating features. In *Proceedings of the IEEE International Conference on Computer Vision*, pp. 3018–3027, 2017.
- Kaiming He, Xiangyu Zhang, Shaoqing Ren, and Jian Sun. Deep residual learning for image recognition. In *Proceedings of the IEEE conference on computer vision and pattern recognition*, pp. 770–778, 2016.
- Martin Heusel, Hubert Ramsauer, Thomas Unterthiner, Bernhard Nessler, Günter Klambauer, and Sepp Hochreiter. Gans trained by a two time-scale update rule converge to a nash equilibrium. *CoRR*, abs/1706.08500, 2017. URL <http://arxiv.org/abs/1706.08500>.
- Jonathan Ho, Ajay Jain, and Pieter Abbeel. Denoising diffusion probabilistic models. *Advances in Neural Information Processing Systems*, 33:6840–6851, 2020.
- Yan Hong, Li Niu, Jianfu Zhang, and Liqing Zhang. Matchinggan: Matching-based few-shot image generation. In *2020 IEEE International Conference on Multimedia and Expo (ICME)*, pp. 1–6. IEEE, 2020a.

- Yan Hong, Li Niu, Jianfu Zhang, Weijie Zhao, Chen Fu, and Liqing Zhang. F2gan: Fusing-and-filling gan for few-shot image generation. In *Proceedings of the 28th ACM International Conference on Multimedia*, pp. 2535–2543, 2020b.
- Tero Karras, Samuli Laine, and Timo Aila. A style-based generator architecture for generative adversarial networks. *arXiv preprint arXiv:1812.04948*, 2018.
- Tero Karras, Miika Aittala, Janne Hellsten, Samuli Laine, Jaakko Lehtinen, and Timo Aila. Training generative adversarial networks with limited data. *Advances in Neural Information Processing Systems*, 33:12104–12114, 2020.
- Diederik P Kingma and Jimmy Ba. Adam: A method for stochastic optimization. *arXiv preprint arXiv:1412.6980*, 2014.
- Alex Krizhevsky, Ilya Sutskever, and Geoffrey E Hinton. Imagenet classification with deep convolutional neural networks. *Advances in neural information processing systems*, 25, 2012.
- Tuomas Kynkäänniemi, Tero Karras, Samuli Laine, Jaakko Lehtinen, and Timo Aila. Improved precision and recall metric for assessing generative models. *Advances in Neural Information Processing Systems*, 32, 2019.
- Yann LeCun, Yoshua Bengio, and Geoffrey Hinton. Deep learning. *nature*, 521(7553):436–444, 2015.
- Kai Li, Yulun Zhang, Kunpeng Li, and Yun Fu. Adversarial feature hallucination networks for few-shot learning. In *Proceedings of the IEEE/CVF Conference on Computer Vision and Pattern Recognition*, pp. 13470–13479, 2020.
- Qi Li, Long Mai, and Anh Nguyen. Improving sample diversity of a pre-trained, class-conditional GAN by changing its class embeddings. *CoRR*, abs/1910.04760, 2019. URL <http://arxiv.org/abs/1910.04760>.
- Weixin Liang, Zixuan Liu, and Can Liu. Dawson: A domain adaptive few shot generation framework. *arXiv preprint arXiv:2001.00576*, 2020.
- Emile Mathieu, Tom Rainforth, Nana Siddharth, and Yee Whye Teh. Disentangling disentanglement in variational autoencoders. In *International Conference on Machine Learning*, pp. 4402–4412. PMLR, 2019.
- Takeru Miyato and Masanori Koyama. cgans with projection discriminator. *arXiv preprint arXiv:1802.05637*, 2018.
- Sangwoo Mo, Minsu Cho, and Jinwoo Shin. Freeze discriminator: A simple baseline for fine-tuning gans. *CoRR*, abs/2002.10964, 2020. URL <https://arxiv.org/abs/2002.10964>.
- Sachin Ravi and Hugo Larochelle. Optimization as a model for few-shot learning. 2016.
- Esther Robb, Wen-Sheng Chu, Abhishek Kumar, and Jia-Bin Huang. Few-shot adaptation of generative adversarial networks. *arXiv preprint arXiv:2010.11943*, 2020.
- Tim Sainburg, Marvin Thielk, Brad Theilman, Benjamin Migliori, and Timothy Gentner. Generative adversarial interpolative autoencoding: adversarial training on latent space interpolations encourage convex latent distributions. *arXiv preprint arXiv:1807.06650*, 2018.
- Jascha Sohl-Dickstein, Eric Weiss, Niru Maheswaranathan, and Surya Ganguli. Deep unsupervised learning using nonequilibrium thermodynamics. In *International Conference on Machine Learning*, pp. 2256–2265. PMLR, 2015.
- Yang Song, Jascha Sohl-Dickstein, Diederik P Kingma, Abhishek Kumar, Stefano Ermon, and Ben Poole. Score-based generative modeling through stochastic differential equations. *arXiv preprint arXiv:2011.13456*, 2020.
- Kumar Sricharan, Raja Bala, Matthew Shreve, Hui Ding, Kumar Saketh, and Jin Sun. Semi-supervised conditional gans. *arXiv preprint arXiv:1708.05789*, 2017.
- Nitish Srivastava, Geoffrey Hinton, Alex Krizhevsky, Ilya Sutskever, and Ruslan Salakhutdinov. Dropout: a simple way to prevent neural networks from overfitting. *The journal of machine learning research*, 15(1):1929–1958, 2014.
- Flood Sung, Yongxin Yang, Li Zhang, Tao Xiang, Philip HS Torr, and Timothy M Hospedales. Learning to compare: Relation network for few-shot learning. In *Proceedings of the IEEE conference on computer vision and pattern recognition*, pp. 1199–1208, 2018.

- Chuanqi Tan, Fuchun Sun, Tao Kong, Wenchang Zhang, Chao Yang, and Chunfang Liu. A survey on deep transfer learning. In *International conference on artificial neural networks*, pp. 270–279. Springer, 2018.
- Vikas Verma, Alex Lamb, Christopher Beckham, Amir Najafi, Ioannis Mitliagkas, David Lopez-Paz, and Yoshua Bengio. Manifold mixup: Better representations by interpolating hidden states. In *International Conference on Machine Learning*, pp. 6438–6447. PMLR, 2019a.
- Vinay Kumar Verma, Dhanajit Brahma, and Piyush Rai. A meta-learning framework for generalized zero-shot learning. *arXiv preprint arXiv:1909.04344*, 2019b.
- Oriol Vinyals, Charles Blundell, Timothy Lillicrap, Daan Wierstra, et al. Matching networks for one shot learning. *Advances in neural information processing systems*, 29:3630–3638, 2016.
- Yaqing Wang, Quanming Yao, James T Kwok, and Lionel M Ni. Generalizing from a few examples: A survey on few-shot learning. *ACM Computing Surveys (CSUR)*, 53(3):1–34, 2020.
- Yu-Xiong Wang, Ross Girshick, Martial Hebert, and Bharath Hariharan. Low-shot learning from imaginary data. In *Proceedings of the IEEE conference on computer vision and pattern recognition*, pp. 7278–7286, 2018.
- Davis Wertheimer, Omid Poursaeed, and Bharath Hariharan. Augmentation-interpolative autoencoders for unsupervised few-shot image generation. *arXiv preprint arXiv:2011.13026*, 2020.
- Zhisheng Xiao, Karsten Kreis, and Arash Vahdat. Tackling the generative learning trilemma with denoising diffusion gans. *CoRR*, abs/2112.07804, 2021. URL <https://arxiv.org/abs/2112.07804>.
- Hongyi Zhang, Moustapha Cisse, Yann N Dauphin, and David Lopez-Paz. mixup: Beyond empirical risk minimization. *arXiv preprint arXiv:1710.09412*, 2017.
- Ruixiang Zhang, Tong Che, Zoubin Ghahramani, Yoshua Bengio, and Yangqiu Song. Metagan: An adversarial approach to few-shot learning. *Advances in neural information processing systems*, 31, 2018.
- Yu Zhang and Qiang Yang. A survey on multi-task learning. *arXiv preprint arXiv:1707.08114*, 2017.

S7 APPENDIX

S7.1 ADDITIONAL FIGURES

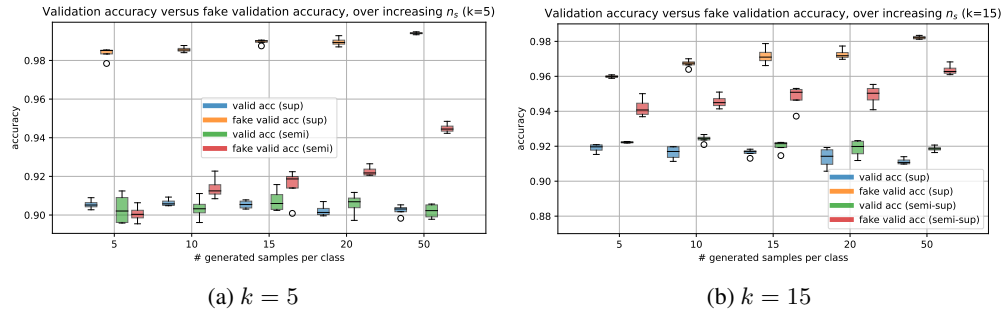


Figure S8: Boxplot showing validation accuracy (blue = supervised, green = semi-supervised) and fake validation accuracy (orange = supervised, red = semi-supervised) for different numbers of generated samples per class n_s . The semi-supervised variant is that described in Equation 5. Fake validation accuracy is a held-out validation set generated by the GAN. It can be seen that as n_s increases, the actual validation accuracy (blue) decreases and fake validation accuracy increases (orange), but this effect is mitigated for the corresponding semi-supervised distributions (shown in green for validation accuracy and red for fake validation accuracy). Results are shown over one dataset seed, with each boxplot being a distribution over the different sampling runs.

S7.2 ADDITIONAL RESULTS

Table S3: Results of $k = 25$ experiments on both $\mathcal{D}_{\text{valid}}$ and $\mathcal{D}_{\text{test}}$. For each experiment and its dataset seed, the hyperparameters used for the test set evaluation correspond to the optimal hyperparameters found for the same corresponding experiment / seed on the validation set (e.g. # of epochs, α for input mixup, n_s for GAN).

	Method	$\mathcal{D}_{\text{valid}}$	$\mathcal{D}_{\text{test}}$
ours	Baseline w/ data aug	93.88 \pm 3.75	93.39 \pm 3.99
	Fine-tuned GAN	93.85 \pm 3.61	93.29 \pm 3.86
	+ semi-supervised (Sec. 5)	94.10 \pm 3.53	93.62 \pm 3.80

S7.3 OPTIMAL HYPERPARAMETERS FOR GAN FINE-TUNING

In order of dataset seeds 0-4:

S7.3.1 $\kappa=5$

- dfm : ['all', 'embed', 'linear', 'all', 'all']
- gfm : ['embed', 'embed', 'embed', 'embed', 'embed']
- γ : [100.0, 100.0, 100.0, 100.0, 100.0]

S7.3.2 $\kappa=10$

- dfm : ['all', 'all', 'all', 'all', 'all']
- gfm : ['embed', 'linear', 'linear', 'embed', 'embed']
- γ : [100.0, 100.0, 100.0, 100.0, 100.0]

S7.3.3 $\kappa=15$

- dfm : ['all', 'linear', 'all', 'linear', 'all']
- gfm : ['embed', 'embed', 'linear', 'embed', 'embed']
- γ : [100.0, 100.0, 100.0, 100.0, 100.0]

S7.4 OPTIMAL HYPERPARAMETERS FOR CLASSIFIER FINE-TUNING

S7.4.1 $\kappa=5$

In order of dataset seeds 0-4:

- **Baseline:** minScale = [0.6, 0.2, 0.8, 0.6, 0.8], 0.60 ± 0.22
- **Input mixup:** α = [0.1, 0.1, 0.1, 0.1, 0.1], 0.10 ± 0.00
- **Fine-tuned GAN:** n_s = [15, 5, 5, 10, 20], 11.00 ± 5.83
- **Semi-supervised:** n_s = [50, 10, 50, 20, 10], 28.00 ± 18.33

S7.4.2 $\kappa=10$

- **Baseline:** minScale = [0.8, 0.6, 0.8, 0.4, 0.6], 0.64 ± 0.15
- **Input mixup:** α = [0.1, 0.1, 0.1, 0.1, 0.1], 0.10 ± 0.00
- **Fine-tuned GAN:** n_s = [5, 10, 10, 20, 15], 12.00 ± 5.10
- **Semi-supervised:** n_s = [10, 10, 20, 50, 50], 28.00 ± 18.33

S7.4.3 $\kappa=15$

- **Baseline:** minScale = [0.8, 0.4, 0.8, 0.8, 0.4], 0.64 ± 0.20
- **Input mixup:** α = [0.1, 0.1, 0.1, 0.1, 0.1], 0.10 ± 0.00
- **Fine-tuned GAN:** n_s = [5, 5, 10, 10, 20], 10.00 ± 5.48
- **Semi-supervised:** n_s = [20, 20, 20, 20, 50], 26.00 ± 12.00

S7.5 GENERATED IMAGES (SOURCE CLASSES)

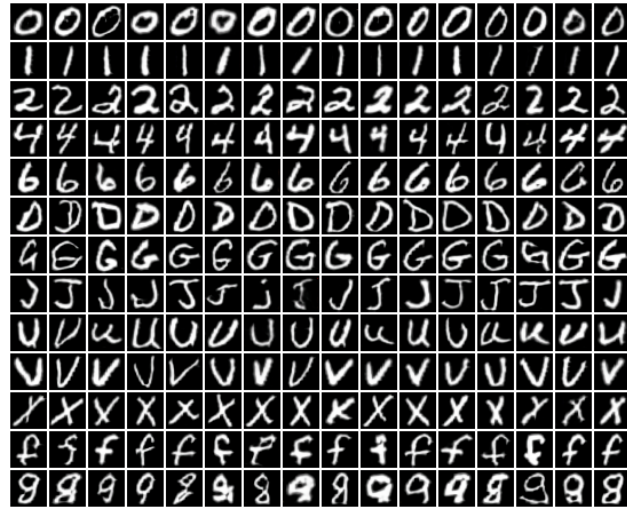


Figure S9: GAN-generated images from the training (source) classes. See Section 2.2 for more information.

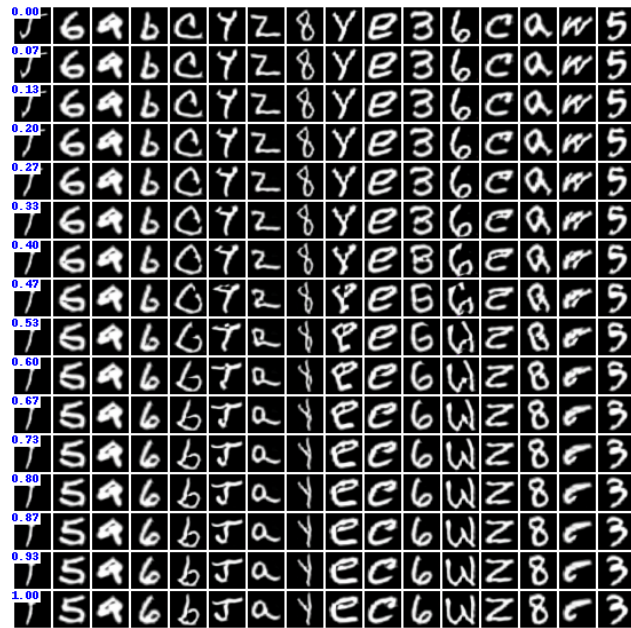
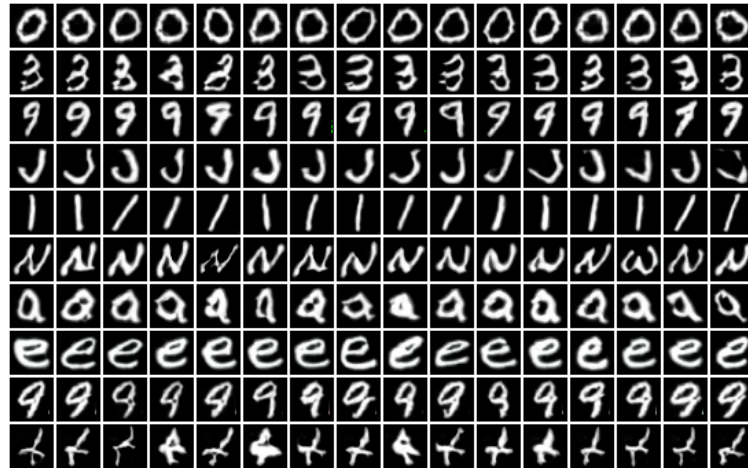
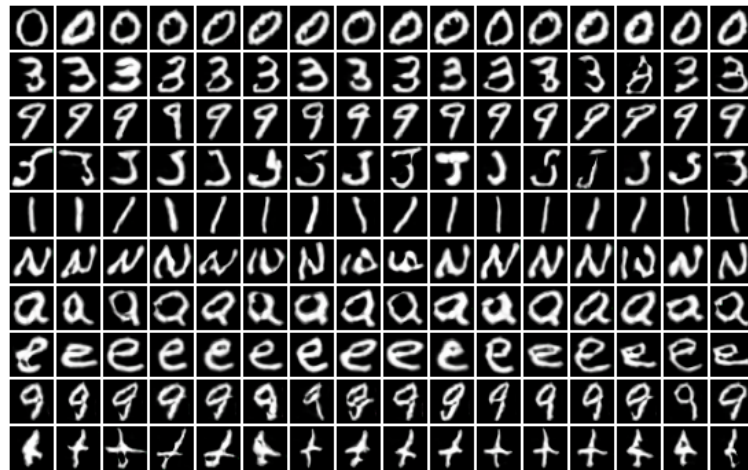


Figure S10: Training class interpolations using the GAN. This is done by interpolating pairs of class embeddings for each embedding layer in the generator network (one per residual block). The top and bottom-most rows consist of randomly selected classes in the training set, and rows in between correspond to interpolations $\alpha \cdot \text{embed}_i(\mathbf{y}_1) + (1 - \alpha) \cdot \text{embed}_i(\mathbf{y}_2)$, where i denotes the i 'th residual block of the generator. Text labels show in blue denote α .

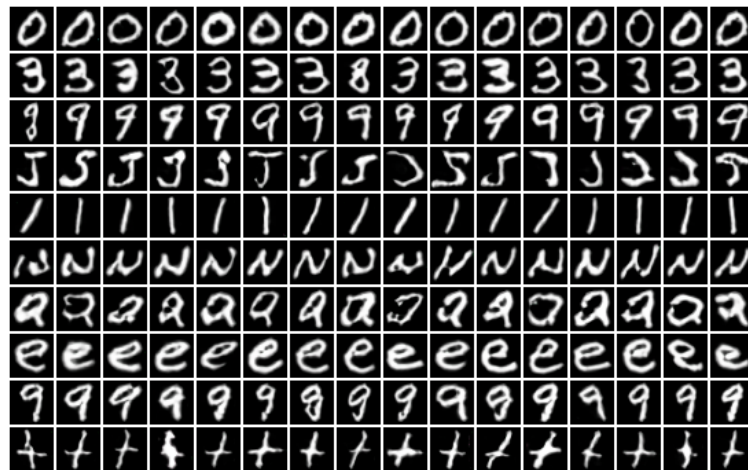
S7.6 GENERATED IMAGES (NOVEL CLASSES)



(a) $k = 5$



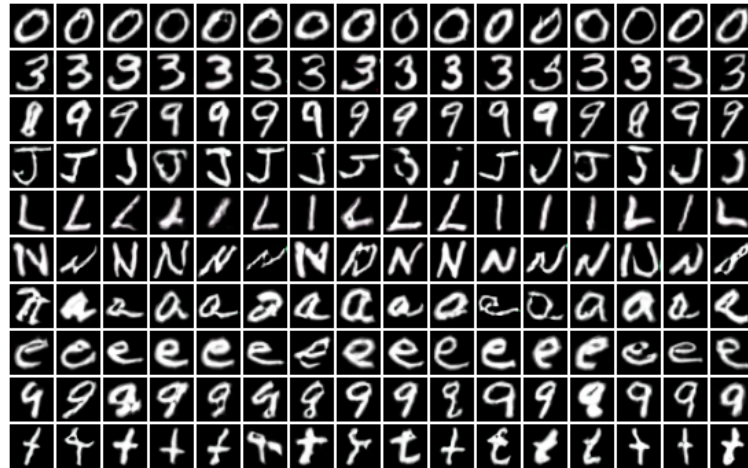
(b) $k = 10$



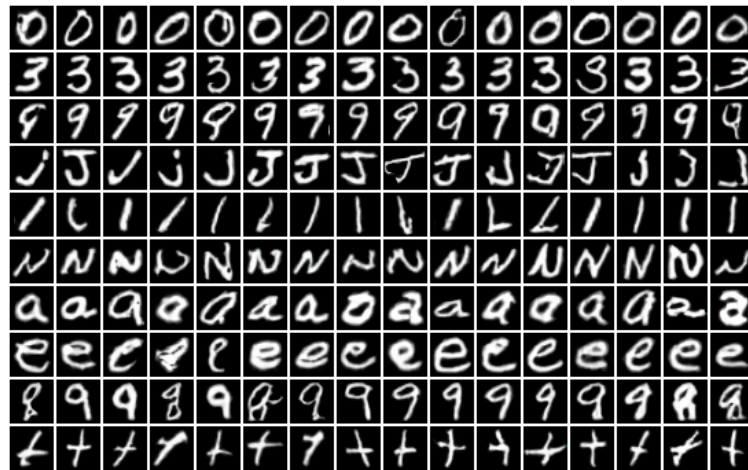
(c) $k = 15$

Figure S11: Generated samples from fine-tuned GAN in Section 2.3.

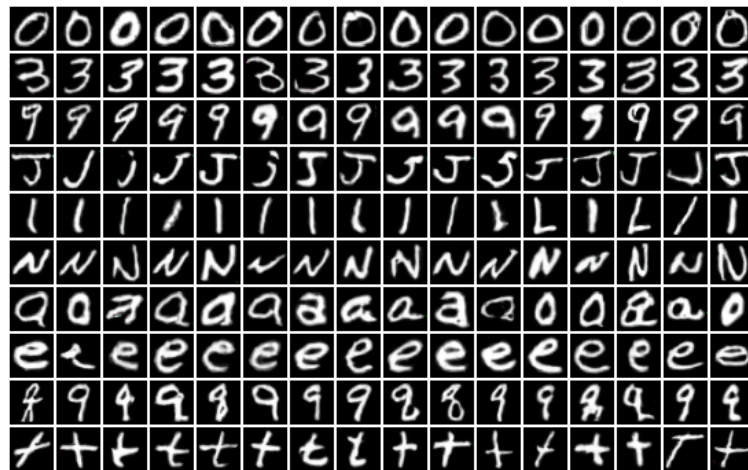
S7.7 GENERATED IMAGES (NOVEL CLASSES, SEMI-SUPERVISED)



(a) $k = 5$



(b) $k = 10$



(c) $k = 15$

Figure S12: Generated samples using the semi-supervised formulation in Section 5.

S7.8 DATASET SPLITS

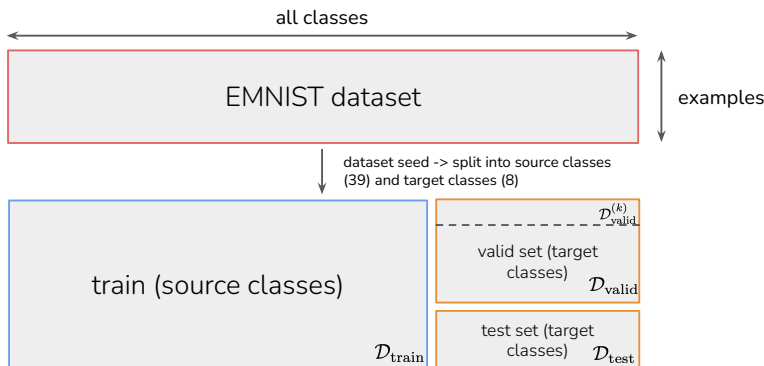


Figure S13: Illustration of how we split our dataset. The dataset seed is used to control what classes comprise training (source) classes and validation/test (target) classes. The GAN and classifier are trained on $\mathcal{D}_{\text{train}}$. The GAN is then fine-tuned on $\mathcal{D}_{\text{valid}}^{(k)}$ and is used to generate examples for the target classes. The classifier pretrained on $\mathcal{D}_{\text{train}}$ is now fine-tuned on $\mathcal{D}_{\text{valid}}^{(k)}$ and the GAN-generated examples and the goal is to maximise performance on $\mathcal{D}_{\text{valid}}$, which is done through hyperparameter tuning. When this is completed, classifier performance is evaluated on the held-out test set $\mathcal{D}_{\text{test}}$.

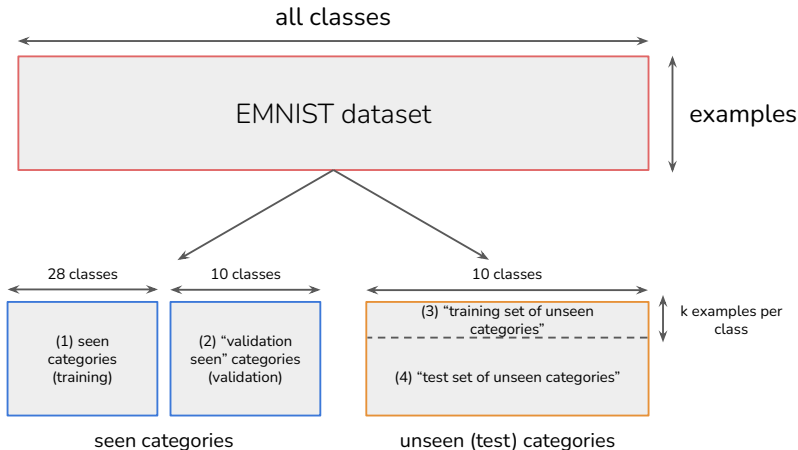


Figure S14: Illustration of how the dataset is split according to MatchingGAN (Hong et al., 2020a). The training set (1) is used to train the GAN, and validation set (2) is used to monitor GAN training (tune GAN training hyperparameters via FID?). What we call the ‘support set’ they have called the ‘training set of unseen categories’ (3), and this is what the GAN uses to generate additional examples. The classifier pre-trained on (1) is now fine-tuned on (3) + the GAN-generated examples and is used to predict accuracy on (4). As we mentioned in Section 4, hyperparameter tuning of the generation process / classifier can lead to biased estimates of performance on (4), since there is no additional held-out test set. Furthermore, in F2GAN (Hong et al., 2020b) no validation set appears to be mentioned.

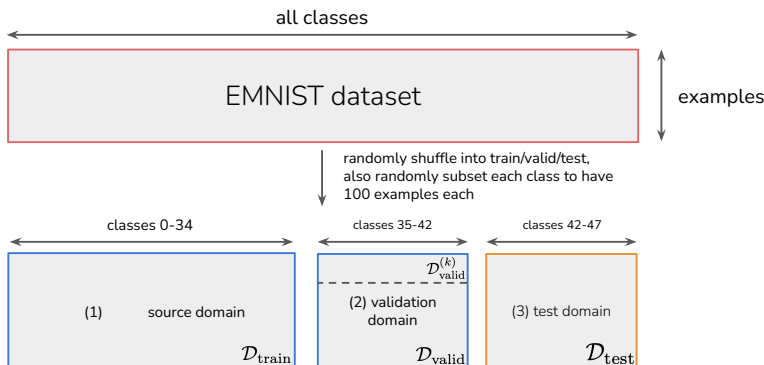


Figure S15: Illustration of how the dataset is split according to DAGAN (Antoniou et al., 2017). Some details regarding the evaluation were not clear, but from what can be gathered, DAGAN is trained on the source domain (training set). A baseline classifier is also trained (from scratch, not fine-tuned) on the validation domain, and hyperparameter tuning is done for n_s to determine how many DAGAN-generated samples per class are optimal. The final evaluation is then training a classifier from scratch on the target domain with the optimal n_s found via hyperparameter tuning. The test accuracy is averaged over five independent runs (dataset seeds).

S7.9 SEMI-SUPERVISED EXPERIMENTS

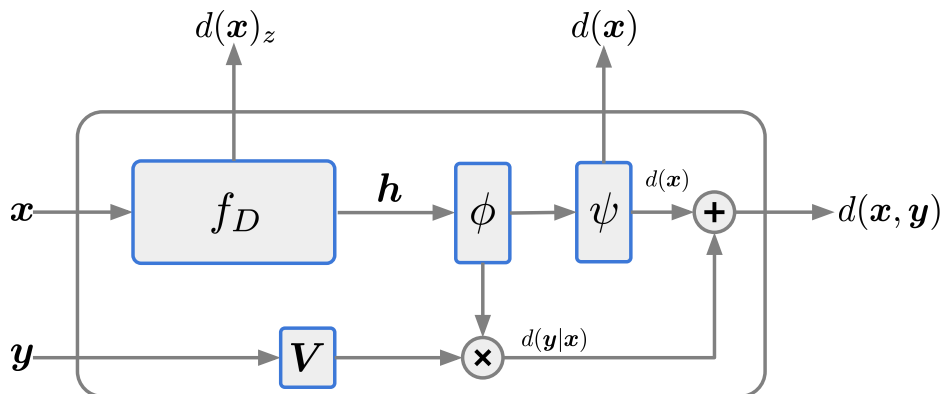


Figure S16: Projection discriminator from Miyato & Koyama (2018). Recall from Section 5 that the output of the discriminator is $d(x, y) = d(y|x) + d(x) = \mathbf{y}^T \mathbf{V} \cdot \phi(f_D(x)) + \psi(\phi(f_D(x)))$. The fact that $d(x, y)$ partly decomposes into $d(x)$ means that the projection discriminator can be leveraged in a semi-supervised manner.